Proceedings of the ASME 2012 International Design Engineering Technical Conferences & Computers and Information in Engineering Conference
IDETC/CIE 2012
August 12-15, 2012, Chicago, IL, USA

DETC2012-70228

INVESTIGATION OF PROTEIN/LIPID INTERACTIONS VIA SCANNING PROBE ACCELERATION MICROSCOPY: THEORY AND EXPERIMENT

Justin Legleiter
Assistant Professor
West Virginia University
Department of Chemistry
Morgantown, WV, USA
justin.legleiter@mail.wvu.edu

Kathleen A. Burke
Graduate Student
West Virginia University
Department of Chemistry
Morgantown, WV, USA

Elizabeth A. Yates
Graduate Student
West Virginia University
Department of Chemistry
Morgantown, WV, USA

ABSTRACT

There is great interest in the application of proximal probe techniques to simultaneously image and measure mechancial properties of surfaces with nanoscale spatial resolution. There have been several innovations in generating time-resolved force interaction between the tip and surface while acquiring a tapping mode AFM image. These tip/sample forces contain information regarding mechanical properties of surfaces in an analogous fashion to a force curve experiment. Here, we demonstrate, via simulation, that the maximum and minimum tapping forces change with respect to the Young's modulus and adhesiveness of a surface, but the roughness of the surfaces has no effect on the tapping forces. Using these changes in tapping forces, we determine the mechanical changes of a lipid membrane after exposure to a huntingtin exon1 (htt exon1) protein with an expanded polyglutamine (polyQ) domain. Expanded polyQ domains in htt is associated with Huntington's disease, a genetic neurodegenerative disorder. The htt exon1 protein caused regions of increased surface roughness to appear in the lipid membrane, and these areas were associated with decreased elasticity and adhesion to the AFM probe.

1. INTRODUCTION

A number of systemic and neurodegenerative disorders, including Alzheimer's disease (AD), Huntington's disease (HD) and Parkinson's disease (PD), are characterized by the accumulation of nanoscale protein aggregates. Most disease-associated protein aggregates contain extended, β-sheet-rich, proteinaceous fibrillar structures, which often have globular, soluble protein aggregate precursors, such as potentially toxic oligomers. Mutations which cause an expansion of CAG triplet repeats encoding polyglutamine (polyQ) are responsible for the subsequent misfolding of specific proteins that contribute directly to the pathogenesis of neurodegenerative disorders, including Huntington's disease (HD) and the spinocerebellar ataxias (SCAs). One of the prototype aggregating proteins that has been extensively studied is exon1 of the huntingtin (htt) protein, strongly implicated in HD, which contains a prototype expanded polyQ domain. Precisely how aggregates comprised of htt with expanded polyQ are toxic to neural cells, leading to the extensive cellular destruction that is the hallmark of HD, remains unclear. The subcellular localization and interaction of htt containing expanded polyQ domains with membranous surfaces comprised of lipid bilayers has been well documented [1-4], and suggests that these interactions may play a causative role in HD pathogenesis.

In this study, we used scanning probe acceleration microscopy (SPAM) to study the mechanical impact on lipid bilayers of a htt exon1 protein with a polyQ domain of 51 repeat units (from here on referred to as HD51Q). While tapping mode AFM has long been established as a non-invasive, high resolution imaging technique, instantaneous tip/sample forces also provide information on local surface properties such as adhesion, rigidity, energy dissipation, and compressibility. SPAM is a technique to recover the instantaneous tip/sample force by taking the second derivative of the cantilever deflection signal after Fourier transform based filtering [5]. SPAM is capable of operating in aqueous solution, making it highly suitable for this study. The SPAM technology combines the non-destructive high resolution imaging of tapping mode AFM with the measurement of local surface properties. Due to its basis in tapping mode, SPAM is nondestructive while maintaining high spatial resolution, both of which are vital in dynamically studying biological surfaces.

We also present a variety of simulations of the entire process of obtaining an AFM image, which allow for the interpretation of SPAM data.

2. METHODS

2.1 Simulation

To determine the impact of surface properties on the tip/sample force interaction during imaging in the tapping mode in fluids, numerical simulations were performed with the aid of MATLAB and SIMULINK (Math Works Inc. Natick, MA.). The cantilever was treated as a point mass and modeled as a single degree of freedom damped driven harmonic oscillator [6, 7].

$$m_{eff}\ddot{z} + b\dot{z} + k[z - D_0 + a_0 \sin(\omega t)] = F_{ext} \quad (1)$$

where m_{eff} is the effective mass of a cantilever, b is the damping coefficient, k is the cantilever spring constant, a_0 is the drive amplitude, ω is the drive frequency, D_0 is the resting position of the cantilever base, F_{ext} is the tip/sample force, and z is the position of the cantilever with respect to the surface. As the cantilever oscillates, the separation distance between the tip and surface changes, and the tip briefly contacts (or taps) the surface during each cycle. As a result, two tip/sample interactions regimes are required to model tapping mode AFM. The first regime is when the tip is not in contact with the surface, and the second is when the tip is in contact with the surface during the tapping event. For the noncontact regime, the external force was approximated using the van der Waals interaction between a sphere and flat surface [8]:

$$F_{ext} = -\frac{HR_{tip}}{6z^2} \quad \text{for } z > a_{DMT}\,, \quad (2)$$

where H is the Hamaker constant, R_{tip} is the tip radius, and a_{DMT} is the interatomic distance parameter of a Derjaguin-Muller-Toporov (DMT) potential [9]. When the separation distance between the tip and surface is less than or equal to the interatomic distance (a_{DMT}), the tip is considered to be in contact with the surface, and the tip/sample force is modeled with a DMT potential,

$$F_{ext} = \frac{4}{3\pi\kappa_{eff}}\sqrt{R}(a_{DMT} - z)^{3/2} - \frac{HR_{tip}}{6{a_{DMT}}^2} \quad for\ z \le a_{DMT} \quad (3)$$

With

$$\kappa_{eff} = \frac{1-{\upsilon_{tip}}^2}{\pi E_{tip}} + \frac{1-{\upsilon_{sample}}^2}{\pi E_{sample}} \quad (4)$$

where E_{tip}, ν_{tip} and E_{sample}, ν_{sample} are, respectively, the Young's modulus and Poisson coefficient of the tip and the sample.

In order to simulate the entire scanning process in an AFM experiment, the model was equipped with a feedback loop containing an integral gain. As the deflection of the cantilever, rather than the position, is the experimentally accessible signal, the deflection (y) of the cantilever was monitored by the feedback loop. The deflection is related to the position by:

$$y = z - D_0 + a_0 \sin(\omega t). \quad (5)$$

The feedback loop was implemented by measuring the amplitude of the deflection signal, comparing it to the specified set point, and adjusting the cantilever position relative to the surface to maintain the set point. The feedback loop feature can be used to simulate the process of acquiring an AFM scan line in which the surface topography can be changed. The Young's modulus can also be changed during a simulated scan line by using Equation 4 to change the output from Equation 3. Changes in the adhesive properties of a surface can be modeled by adjusting the Hamaker constant in Equations 2 and 3 because the Hamaker constant is related to the surface free energy (γ) between two materials by:

$$\gamma = \frac{H}{24\pi a_{DMT}} \approx \frac{H}{2.1\times10^{-21}}\,. \quad (6)$$

All of these changes can by synchronized with changes in topography.

2.2 Experiment

Supported lipid bilayer formation. Bilayers used in this study were produced though the fusion of TBLE vesicles on mica. Total brain lipid extract (porcine) was purchased from Avanti Polar Lipids (Alabaster, AL), dried under a nitrogen stream, lyophilized, and resuspended in PBS (pH 7.3) at a concentration of 1 mg/ml. Using an acetone/dry ice bath, bilayers and multilayer lipid sheets were formed by five cycles of freeze-thaw treatment [10, 11]. The lipid suspensions were then sonicated for 15 minutes to promote vesicle formation. The vesicles were then injected into an AFM fluid cell and allowed to deposit and fuse into a defect free supported lipid bilayer on a cleaved mica sustrate. Only defect free bilayers were used in this study.

Protein preparation. GST-HD51Q fusion proteins were purified as described (52). Cleavage of the GST moiety by PreScission Protease (Amersham Biosciences) initiates aggregation. Fresh, unfrozen GST-HD51Q was used for each experiment. GST-HD51Q was centrifuged at 20,000 x *g* for 30 min at 4 °C to remove any preexisting aggregates before the addition of the PreScission protease. After adjusting the final concentration to 20 µM, PreScission protease was added to the GST-HD51Q, and the solution was allowed to incubate on ice for one hour before the cleaved protein was injected into the AFM fluid cell containing preformed supported lipid bilayers.

AFM imaging conditions. In situ AFM experiments were preformed with a Nanoscope V Multimode scanning probe microscope (Bruker, Santa Barbara, CA) that was equipped with a tapping fluid cell. V-shaped silicon nitride cantilevers with a nominal spring constant of 0.27 N/m were used. Typical

imaging parameters were scan rates of 1.95 Hz, cantilever drive frequencies ranging from approximately 8-9 kHz, and set-point ratio of 0.7. Images were captured at 5 x 20 μm and 128 x 512 pixel resolution.

SPAM analysis was used to reconstruct every tapping event during AFM imaging as described [5]. For this analysis, cantilever deflection trajectories were captured during imaging using a signal access module (Bruker), a CompuScope 14-Bit A/D Octopus data acquisition card (Gage Applied Technologies, Lachine, QB, Canada), and custom-written software. Trajectories were sampled at 2–5 MS/s with 14-bit resolution. The trajectory of the cantilever was filtered using a Fourier transform based harmonic comb filter, and the second derivative of the filtered cantilever deflection trajectory is taken and multiplied by the effective mass, m_{eff}, of the cantilever to obtain the time-resolved based tapping force between the tip and sample.

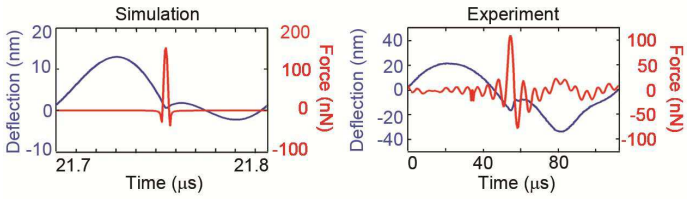

Figure 1. Experimental and simulated AFM cantilever trajectories and tip/sample forces. Cantilever deflection trajectories are presented in blue; while, the tip/sample force interactions are presented in red.

3. RESULTS AND DISCUSSION

To determine the impact of surface mechanical properties on specific features of time-resolved tapping forces, simulations were performed with parameters based on the typical experimental parameters of an *in situ* tapping mode AFM experiment. These parameters included: drive frequency of 8-10 kHz, spring constant of 0.5 N/m, free amplitude of 15 nm, a set point ratio of 0.7, and a quality factor of 2. Using these parameters, the model is capable of capturing the features of the cantilever deflection trajectory and tip/sample force interaction in real tapping mode AFM experiments (Figure 1) [12]. Two features of the tip/sample force interactions that will be monitored are the maximum tapping force (F_{max}) and minimum tapping force (F_{min}). F_{max} is defined as the peak or largest positive force experienced between the tip and surface, and F_{min} per oscillation cycle is defined as the peak or largest negative force experienced between the tip and surface. It has been demonstrated that higher modes, especially the second, of the cantilever can contribute to cantilever motion near surfaces in fluids [13]. Ignoring these higher modes have proven to be sufficient for understanding some features of tapping forces in solution [14], abd the resulting error in the forces has been estimated to be ~10-15% [13].

The rigidity of the model surface can be modulated by changing the Young's modulus of the sample (E_{sample} in Equation 4). As the Young's modulus of the sample increased from 0.5 to 5 GPa, changes in F_{max} and F_{min} were observed (Figure 2). Increasing E_{sample} causes the surface to be less compliant, and the constant, κ_{eff} in equation 3, to be smaller. As a result the F_{max} observed for each tapping event increases in magnitude with an increasing E_{sample}, and this relationship follows a power law (Figure 2B). However, F_{min} is unaffected by changes in E_{sample} (Figure 2C). As the surface free energy (and adhesive force) between the tip and surface are related to the Hamaker constant by Equation 6, simulations were run with a variety of Hamaker constants. As the Hamaker constant increased from 0.1 to 1.75 aJ, changes in F_{max} and F_{min} were observed (Figure 3). Increasing the Hamaker constant causes a larger attractive component to the force between the tip and surface, resulting in the tip pushing further into the surface. Due to pushing further into the surface, the Hertzian portion of the tip/sample force in the contact regime increases, and a net increase in the F_{max} is observed. This increase in the magnitude of F_{max} has a linear relationship with the Hamaker constant (Figure 3B). The magnitude of F_{min} also increases linearly with an increasing Hamaker constant, as the attractive component of the tip/sample force increases (Figure 3C). Collectively, the simulations with varying values of the Hamaker constant or Young's modulus demonstrate that unique features of the tip/sample tapping force can be used to determine relative changes in the mechanical properties of a surface.

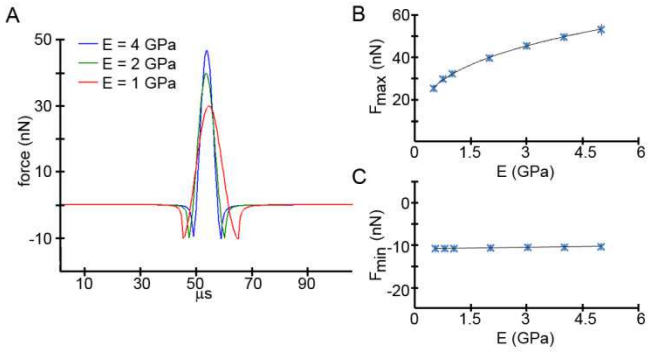

Figure 2. The dependence of tapping forces on surface Young's modulus. (A) Simulated time-resolved tip/sample force interactions with different surface Young's modulus. (B) The maximum tapping force between the tip and surfaces increases with larger Young's moduli with a power law dependence. (C) The minimum tapping force is not dependent on surface Young's modulus.

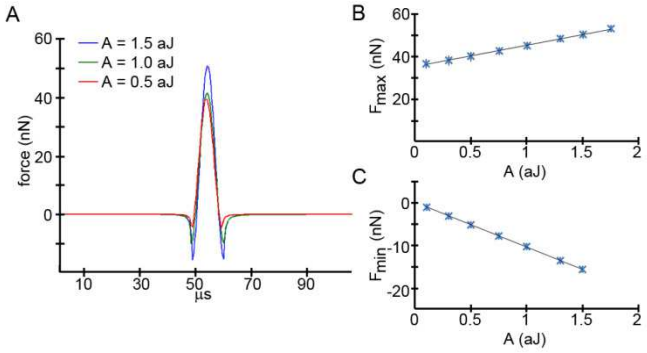

Figure 3. The dependence of tapping forces on the Hamaker constant. (A) Simulated time-resolved tip/sample force interactions with different Hamaker constants. (B) The maximum tapping force between the tip and surfaces increases linearly with increases in the Hamaker constant. (C) The minimum tapping force increases in magnitude (becomes more negative) with increases in the Hamaker constant.

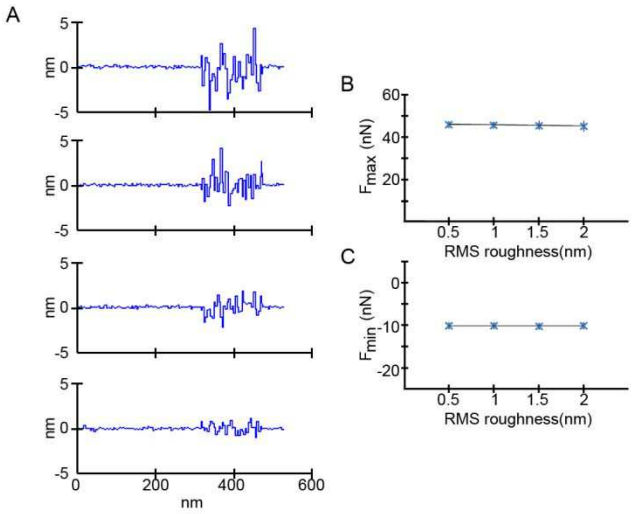

Figure 4. The dependence of tapping forces on RMS surface Roughness. (A) Model surfaces with regions of increased surface roughness were used in simulations of solution tapping mode AFM experiments. (B) The maximum and (C) minimum tapping force between the tip and surfaces was not dependent on the surface roughness.

While F_{max} and F_{min} are affected by changes in the mechanical properties of the surface, the tip/sample tapping force must not be dependent on surface topography or roughness for these changes to be useful in studying surface mechanical properties. To determine the role of surface roughness on F_{max} and F_{min}, a series of simulations were performed with a model surface that consisted of two regions of RMS roughness of 0.1 nm that flanked a region in which the RMS roughness was increased from 0.5 to 2.0 nm in successive simulations (Figure 4A). The height of the surface is adjusted after every oscillation cycle, so a new height is experienced for every tapping event within the range specified by the RMS roughness. Within simulations, F_{max} and F_{min} did not change when the RMS roughness of the model surface was increased (not shown). Across simulations, there was no effect on F_{max} and F_{min} by increasing the RMS roughness of the model surface (Figure 4B-C).

To apply relationships between surface mechanical properties and specific features of the tip/sample force interaction to a real system, we performed SPAM experiments on supported TBLE lipid bilayers that were exposed to an amyloidogenic protein, HD51Q. Initially, when aliquots of freshly prepared solutions of HD51Q were added to the TBLE bilayers (final concentration of protein was 20 μM), discrete patches of increased surface roughness formed on the supported lipid bilayer (Figure 5). These regions represent areas were the lipid bilayer structure had been disrupted by the binding, insertion, and aggregation of HD51Q. A freshly formed bilayer had an RMS surface roughness of ~0.15 nm. After exposure to HD51Q, areas with RMS surface roughness increased to ~1.2 nm, which is within the range of the model surfaces used in simulations (Figure 4). While obtaining the topography images of this protein/bilayer system, the entire cantilever deflection signal was captured and used to reconstruct every tapping event during the imaging process. The F_{max} and F_{min} of each tapping event was then used to reconstruct surface map based on these two specific features of the tip/sample force (Figure 6). Both F_{max} and F_{min} images display strong contrast, and are directly comparable to the topography of the surface. Regions of the bilayer surface where exposure to HD51Q had resulted in increased surface roughness were associated with smaller magntides of F_{max} and F_{min} when compared to unaffected regions of the bilayer, as can be seen in histograms of all of the F_{max} and F_{min} measurements (Figure 6). The topography image can be used as a reference to verify which tapping forces are associated with the different regions of the surface.

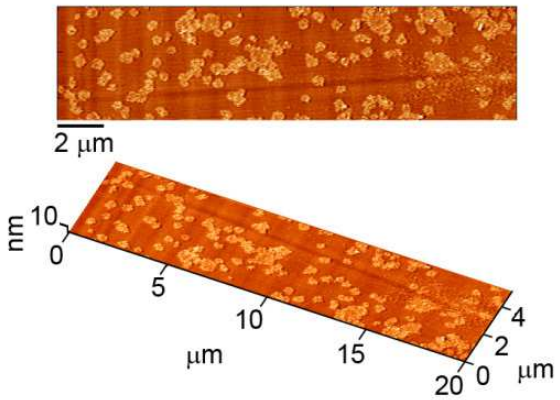

Figure 5. Topography image, both 2D and 3D, of a lipid bilayer that has been exposed to an amyloidogenic HD51Q. Small regions of disrupted bilayer appeared after the addtion of the protein.

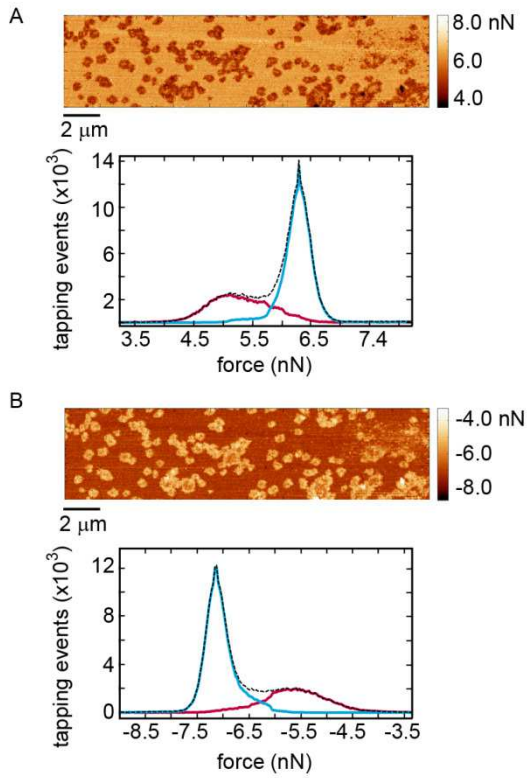

Figure 6. Reconstructed (A) Fmax amd (B) Fmin images with histograms of all the tapping forces directly below each image. In the histograms, the black dotted line represents all of the tapping forces, the blue line represents tapping forces associated with unaffected regions of the bilayer, and the red line represents tapping forces associated with disrupted regions of the bilayer.

Using the results of the simulation, the observed contrast in F_{max} and F_{min} can be used to determine how the interaction of HD51Q altered the mechanical properties of the bilayer. While the protein disrupted the morphology of the bilayer as evidenced by regions of increased surface roughness, this altered morphology would not have resulted in the F_{max} or F_{min} contrast based on simulation. As F_{min} was not altered by changes in the Young's modulus of the surface in simulation, the observed contrast in F_{min} must be due to a decreased adhesive interaction between the tip and the disrupted region of the bilayer. The smaller F_{max} associated with disrupted regions of the bilayer could potentially be caused by both changes in the bilayer's Young's modulus and the Hamaker constant associated with the interaction between the tip and surface. However, the decrease in F_{max} associated with changes in the Hamaker constant can be estimated from the observed change in F_{min} based on simulation results. When doing this analysis, it is apparent that the change in F_{max} cannot be completely accounted for by what would be expected based on the relative shift in F_{min}. Therefore, some of the observed decrease in F_{max} must be associated with a decreased Young's modulus in regions where HD51Q has disrupted the bilayer. Collectively, these results indicate that interaction with HD51Q results in a decreased Young's modulus of the bilayer and a decreased adhesive interaction between the tip and surface. Taking into account the increased roughness of these regions, a potential explanation of these observed changes in the bilayer could be due to the protein altering the packing of the lipid components within the bilayer. This would lead to a rougher surface, a more compressible surface due to less efficient packing, and a decrease in the number of potential hydrogen bonds formed between the tip and bilayer surface.

4. CONCLUSIONS

In the field of scanning probe techniques, there is much interest in the application of methods that simultaneously image and capture mechanical information about surfaces to study biological systems. Presented results and simulations demonstrate that the maximum and minimum observed tapping force for tapping mode AFM operation in fluids is directly related to material properties such as Young's modulus and surface free energy between the tip and surface. These forces are not dependent on the surface morphology. As a result, the mechanical properties of biological surfaces, such as lipid bilayers, can be relatively determined by comparing specific features of the time resolved tip/sample force interaction without having to be concerned about the effect of surface morphology. Based on this principle, we have demonstrated the applicability of the SPAM technique to study changes in lipid bilayers exposed to an amyloidogenic protein. These studies can be extended to a variety of protein interactions with lipid membranes. Proteins that could potentially be studied to determine how they influence lipid membrane properties include other amyloid forming proteins, anti-microbrial peptides, and membrane proteins.

ACKNOWLEDGMENTS

This work was funded by the Brodie Discovery and Innovation fund as well as the National Science Foundation (NSF#1054211).

REFERENCES

[1] Kegel, K., Kim, M., Sapp, E., McIntyre, C., Gastano, J., Aronin, N. and DiFiglia, M., 2000, "Huntingtin expression stimulates endosomal-lysosomal activity, endosome tubulation, and autophagy," J. Neurosci., 20, 7268–7278.
[2] Orr, A. L., Li, S., Wang, C.-E., Li, H., Wang, J., Rong, J., Xu, X., Mastroberardino, P. G., Greenamyre, J. T. and Li, X.-J., 2008, "N-Terminal Mutant Huntingtin Associates with Mitochondria and Impairs Mitochondrial Trafficking," J. Neurosci., 28, 2783-2792.
[3] Qin, Z.-H., Wang, Y., Sapp, E., Cuiffo, B., Wanker, E., Hayden, M., Kegel, K., Aronin, N. and DiFiglia, M., 2004,

"Huntingtin bodies sequester vesicle-associated proteins by a polyproline-dependent interaction," J. Neurosci., 24, 269-281.
[4] Suopanki, J., Götz, C., Lutsch, G., Schiller, J., Harjes, P., Herrmann, A. and Wanker, E. E., 2006, "Interaction of huntingtin fragments with brain membranes – clues to early dysfunction in Huntington's disease," J. Neurochem., 96, 870-884.
[5] Legleiter, J., Park, M., Cusick, B. and Kowalewski, T., 2006, "Scanning probe acceleration microscopy (SPAM) in fluids: mapping mechanical properties of surfaces at the nanoscale," Proc. Nat. Acad. Sci. (USA), 103, 4813-4818.
[6] Kuhle A, H, S. A. and J, B., 1997, "Role of attractive forces in tapping tip force microscopy," J. Appl. Phys., 81, 6562.
[7] Salapaka, M. V., Chen, D. J. and Cleveland, J. P., 2000, "Linearity of amplitude and phase in tapping-mode atomic force microscopy," Phys. Rev. B: Condens. Matter Mater. Phys., 61, 1106-1115.
[8] Israelachvili, J. and Wennerstrom, H., 1996, "Role of hydration and water structure in biological and colloidal interactions," Nature, 379, 219-25.
[9] Derjaguin B V, M. V. M. and P, T. Y., 1975, "Effect of contact deformations on the adhesion of particles," J. Colloid Interface Sci., 53, 314.
[10] Yip, C. M., Elton, E. A., Darabie, A. A., Morrison, M. R. and McLaurin, J., 2001, "Cholesterol, a modulator of membrane-associated Abeta-fibrillogenesis and neurotoxicity," J. Mol. Biol., 311, 723-34.
[11] Yip, C. M. and McLaurin, J., 2001, "Amyloid-beta peptide assembly: a critical step in fibrillogenesis and membrane disruption," Biophys. J., 80, 1359-71.
[12] Legleiter, J. and Kowalewski, T., 2005, "Insights into fluid tapping-mode atomic force microscopy provided by numerical simulations," Appl. Phys. Lett., 87, 163120.
[13] Basak, S. and Raman, A., 2007, "Dynamics of tapping mode atomic force microscopy in liquids: Theory and experiments," Appl. Phys. Lett, 91, 064107.
[14] Xu, X., Carrasco, C., de Pablo, P.J., Gomez-Herrero, J. and Raman, A., 2008, "Unmasking imaging forces on soft biological samples in liquids when using dynamic atomic force microscopy: a case study on viral capsids," Biophys. J., 95, 2520-2528.